Generation of sub-mJ terahertz pulses by optical rectification

J. A. Fülöp,[1,*] L. Pálfalvi,[1] S. Klingebiel,[2] G. Almási,[1] F. Krausz,[2,3] S. Karsch,[2,3] and J. Hebling[1]

[1]Department of Experimental Physics, University of Pécs, Ifjúság ú. 6, H-7624 Pécs, Hungary

[2]Max-Planck-Institut für Quantenoptik, Hans-Kopfermann-Str. 1, D-85748 Garching, Germany

[3]Department für Physik, Ludwig-Maximilians-Universität München, Am Coulombwall 1, D-85748 Garching, Germany

*Corresponding author: fulop@fizika.ttk.pte.hu

Received October 3, 2011; revised December 19, 2011; accepted December 21, 2011;
posted December 23, 2011 (Doc. ID 155578); published February 8, 2012

Recent theoretical calculations predicted an order-of-magnitude increase in the efficiency of terahertz pulse generation by optical rectification in lithium niobate when 500 fs long pump pulses are used, rather than the commonly used ~100 fs pulses. Even by using longer than optimal pump pulses of 1.3 ps duration, 2.5× higher THz pulse energy (125 μJ) was measured with 2.5× higher pump-to-THz energy conversion efficiency (0.25%) than reported previously with shorter pulses. These results verify the advantage of longer pump pulses and support the expectation that mJ-level THz pulses will be available by cooling the crystal and using large pumped area.

OCIS codes: 300.6495, 190.7110, 260.3090.

Intense ultrashort terahertz (THz) pulses are an enabling tool for many new applications. The spectacular increase in the energy of THz pulses in the past few years [1–3] enabled the investigation of nonlinear THz response [4] and ultrafast carrier dynamics in semiconductors by THz pump–THz probe measurements [5–7]. Highly nonlinear THz light-matter interaction in single-walled carbon nanotubes was investigated by THz pump–optical probe spectroscopy [8]. High-field single-cycle THz pulses have been used for bidirectional ultrafast electric-field gating of interlayer charge transport in a cuprate superconductor [9]. Other intriguing new applications require THz field strengths, which are one or two orders of magnitude larger than what is presently available in the frequency range about 1 THz. Examples of such application possibilities are manipulation of molecules by strong (quasistatic) electric fields, enhancement of attosecond pulse generation [10], electron acceleration, undulation, deflection, and spatial as well as temporal focusing [11].

In recent years optical rectification (OR) of femtosecond laser pulses became a widely used method for generation of intense THz pulses. By using ZnTe in collinear geometry pumped by a Ti:sapphire laser up to 1.5 μJ THz energy was generated [1], where the efficiency was limited by free-carrier absorption (FCA) in the THz range caused by two-photon absorption at the pump wavelength. $LiNbO_3$ (LN) has higher nonlinearity, and it can be pumped at higher intensities since only higher-order multiphoton absorption is effective. For phase matching tilted-pulse-front pumping (TPFP) is required [12]. By using this technique up to 50 μJ THz pulse energy [2] and 1.2 MV/cm focused peak electric-field strength [13] was reported, with corresponding pump-to-THz energy conversion efficiencies of 5×10^{-4} and 1×10^{-3}, respectively.

Recently, detailed theoretical analysis of LN-based TPFP sources was given [14–16]. Optimal parameters were given for the pulse-front-tilting setup containing imaging optics to reduce distortions and to allow increasing the pump spot size [14]. It was shown that the THz energy can be increased by two orders of magnitude beyond the state of the art [15]. Three main factors contribute to the predicted increase: (i) longer Fourier-limited (FL) pump pulses, (ii) cooling of the LN crystal to reduce its THz absorption, and (iii) large pump spot size and energy. The typical FL pump pulse duration used in many experiments was about 100 fs [2,6–8,13]. In contrast, calculations predict an optimum FL pump pulse duration of about 500 fs with 6× larger THz-generation efficiency at room temperature than for 100 fs [15]. The main reason for the increased efficiency is the longer effective material length utilized for THz generation [14,15]. It should be emphasized that it is essential to use FL pump pulses rather than temporally stretched broadband pulses [14].

In this letter we report on the generation of THz pulses by OR from a LN-based TPFP source with the highest energy and highest pump-to-THz energy conversion efficiency reported so far by using longer (ps) pump pulses, instead of the commonly used ~100 fs pulses.

A diode-pumped high-energy picosecond Yb:YAG chirped-pulse amplification system was used as the pump laser with 10 Hz repetition rate, 1030 nm central wavelength, and 2.6 nm FWHM spectral bandwidth [17]. The pulses were compressed to about 1.3 ps duration containing a remaining third- (and higher-) order spectral phase. Thus, the pump pulse duration was significantly longer than its FL value and the calculated 500 fs optimum value for THz generation. The maximum available energy was 200 mJ; up to about 70 mJ was used in the experiment.

A TPFP setup with optimized imaging parameters was used for THz generation in a LN crystal [14]. The intensity front of the pump pulses was tilted by a 1400 lines/mm grating and imaged with a 20 cm focal length lens of 25 mm diameter, with a demagnification of 1.7, into the 0.6% MgO-doped stoichiometric LN crystal. A $\lambda/2$ plate was used to rotate the horizontally polarized pump light from the grating to vertical polarization, parallel to the optic axis of the LN crystal. The pump spot size on the crystal surface was 6.8 mm in the horizontal direction and 13.0 mm in the

vertical direction (at $1/e^2$ value of the peak intensity). The LN crystal had a triangular shape in the horizontal plane (see inset of Fig. 3). The size of the input surface was 13×16 mm^2 (horizontal $\times$ vertical), which allowed a maximum pumped area of 8.1×16 mm^2. After losses at the grating and elsewhere, approximately 53 mJ of maximum pump energy reached the crystal. A calibrated pyroelectric detector (Microtech Instruments) with a 2×3 mm^2 active area and a cone-shaped input opening with 15 mm diameter was used for measuring the energy of the THz pulses. Silicon plates were placed in front of the detector in order to attenuate the THz pulses to avoid saturation and to block the optical radiation. The voltage signal of the detector was fed to a storage oscilloscope, and the THz energy E_{THz} was calculated from the voltage modulation V_m of the recorded trace according to $E_{\mathrm{THz}} = C \cdot V_m \cdot \tau/S$, where the sensitivity $S = 700$ V/W was obtained from factory calibration, while the correction factor $C \approx 1$ and the time constant $\tau = 25$ ms were determined from fitting of the recorded trace.

The measured THz energy is shown in Fig. 1 as the function of the pump pulse energy before the LN crystal. A continuous increase in the THz energy can be observed up to about 50 mJ pump energy. The increase of THz energy with increasing pump energy followed a power law with a power dependence of about 1.6 up to above 20 mJ pump energy (dashed black line in Fig. 1). Above this pump level the increase in THz yield was weaker. The maximum THz energy of 125 μJ is reached at 50 mJ pump energy, giving a pump-to-THz energy conversion efficiency of 0.25%. At higher pump energy the decrease of the THz energy was observed. This can be attributed to the occurrence of 4-photon absorption (4 PA) at the pump wavelength and the corresponding increase in FCA in the THz range. The energy conversion efficiency was increasing from 0.08% at 4 mJ pump energy to its maximum of 0.26% at 45 mJ pump energy.

For numerical modeling of the experimental data the wave equation with the nonlinear polarization was solved in the spectral domain. The applied theoretical model, described in detail in Refs. [14,15], takes into account (i) the variation of the pump pulse duration (and therefore of the pump intensity) with the propagation distance owing to material and, more importantly, to angular dispersion, (ii) the noncollinear propagation of pump and THz beams, and (iii) the absorption in the THz range owing to the complex dielectric function (determined by phonon resonances) as well as owing to FCA caused by 4 PA at the pump wavelength [14]. In the calculations we have used the estimated value of 10^{-7} cm^5/GW^3 for the 4 PA coefficient [18]. The deviation of the calculated THz pulse energy values (empty red squares in Fig. 1) from the square law (solid red line) above ~20 mJ pump energy is because of 4 PA. The theoretical curve shows about three times higher maximum THz energy as the measured maximum, whereas the difference decreases with decreasing pump energy. The pump energy corresponding to the calculated maximum THz energy is about 42 mJ, which is in reasonably good agreement with the experimental finding (50 mJ). Because LN has a bandgap of 3.8 eV at room temperature, at the pump wavelength of 1030 nm only 4 PA should be possible in a perfectly pure material. However, impurities can cause 2-photon absorption, which can be a reason for the observed weaker than the square law increase in the THz yield below ~20 mJ pump energy.

The pulse shape was not measured. However, previous experience shows that calculated and measured THz pulse shapes and spectra are in reasonably good agreement [19]. Because of the long pump pulse duration, the peak of the calculated THz spectrum is at the relatively low value of 0.25 THz, where the dispersion of LN is small. Accordingly, the calculated temporal shape of the THz pulses comprised a single oscillation cycle [20].

The measured THz beam profiles in the horizontal plane (in the plane of pump angular dispersion) are shown in Fig. 2 for 2 cm and 22 cm distances behind the output surface of the LN crystal. The measured THz beam diameter is about 33 mm (FWHM) at 22 cm. Assuming plane THz wavefront at the output surface of the crystal gives 1.7× smaller value, 19 mm FWHM, with a Gaussian THz beam waist calculated from the square of the projected input pump beam profile. If the curvature of the THz phase fronts is also taken into account (Fig. 3), which is present even in an optimized pulse-front-tilting setup as predicted by ray-tracing calculations [14], about 33 mm THz FWHM is obtained for the 22 cm

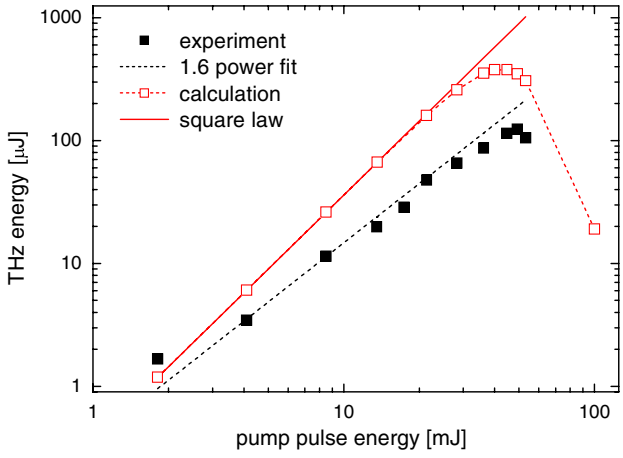

Fig. 1. (Color online) Measured and calculated THz energy versus pump energy.

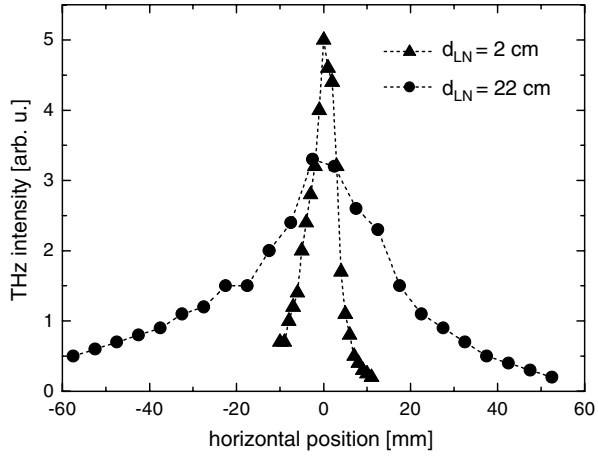

Fig. 2. Measured THz beam profiles in the horizontal plane at 2 cm and 22 cm distances behind the output surface of the LN crystal.

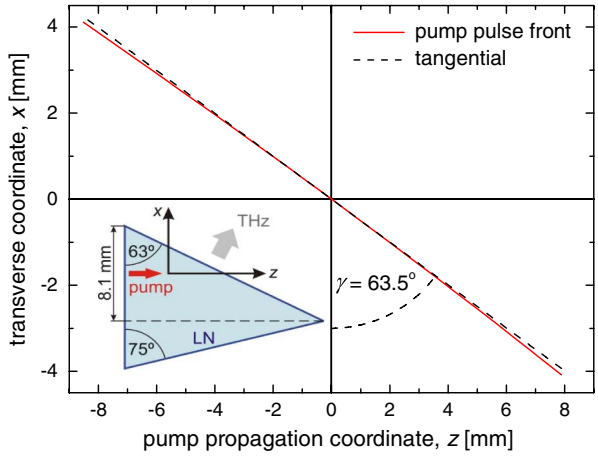

Fig. 3. (Color online) Calculated shape of the tilted pump pulse front inside the LN crystal. Inset: geometry of the LN crystal.

distance, which is in agreement with the experimental finding.

Figure 4 shows the calculated pump-to-THz conversion efficiencies, where the FL pump pulse duration was varied, while its peak intensity was kept at the constant value of 20 GW/cm^2. At room temperature the highest efficiency (2%) is predicted for 500 fs pump pulse duration [15] (red curve with empty squares in Fig. 4). This is about two times higher than the efficiency calculated for 1.3 ps FL pump pulse duration (1.1%). If we also take into account the uncompensated third-order spectral phase present in the experiment, the calculated THz yield gets further reduced to 0.74% (black empty square). The reason for the reduced efficiency is the reduced effective crystal length owing to the larger spectral width. For larger spectral width the angular dispersion introduced by the THz-generation setup causes a faster variation of the pump pulse duration inside the LN crystal [14,15]. The corresponding experimental value (0.22%), obtained with about 21 mJ pump energy, is also shown in Fig. 4.

Even though our pump pulses were longer than optimal, the experimentally obtained THz-generation efficiency (up to 0.25%) was 2.5 times higher than the previously reported highest value [13] and 5× higher than

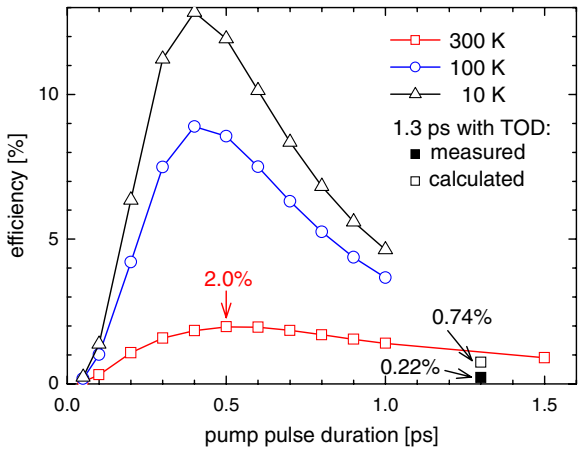

Fig. 4. (Color online) Calculated THz-generation efficiency versus FL pump pulse duration for various crystal temperatures. TOD: third-order phase.

the efficiency for the previously reported highest THz energy [2]. This result clearly shows the prospects of using pump pulses with 500 fs pulse duration for achieving THz pulses with mJ-level energy [15]. The THz-generation efficiency can be improved further by cooling the LN crystal to reduce its absorption (Fig. 4).

In conclusion, THz pulses of the highest so far 125 μJ energy and with the highest 0.25% efficiency were generated by OR of 1.3 ps pulses in LN. Our experimental findings together with theoretical predictions indicate the feasibility of efficient THz pulse generation with mJ-level output energy by using optimal pump pulse duration, cooling the LN crystal, and using a contact grating [14] for TPFP to allow a large pumped area.

Financial support from Hungarian Scientific Research Fund grant numbers 76101 and 78262 and from "Developing Competitiveness of Universities in the South Transdanubian Region" (SROP-4.2.1.B-10/2/KONV-2010-0002) is acknowledged.

References

1. F. Blanchard, L. Razzari, H. C. Bandulet, G. Sharma, R. Morandotti, J. C. Kieffer, T. Ozaki, M. Reid, H. F. Tiedje, H. K. Haugen, and F. A. Hegmann, Opt. Express **15**, 13212 (2007).
2. A. Stepanov, S. Henin, Y. Petit, L. Bonacina, J. Kasparian, and J. P. Wolf, Appl. Phys. B **101**, 11 (2010).
3. Y. Shen, T. Watanabe, D. A. Arena, C.-C. Kao, J. B. Murphy, T. Y. Tsang, X. J. Wang, and G. L. Carr, Phys. Rev. Lett. **99**, 043901 (2007).
4. P. Gaal, K. Reimann, M. Woerner, T. Elsaesser, R. Hey, and K. H. Ploog, Phys. Rev. Lett. **96**, 187402 (2006).
5. L. Razzari, F. H. Su, G. Sharma, F. Blanchard, A. Ayesheshim, H. C. Bandulet, R. Morandotti, J. C. Kieffer, T. Ozaki, M. Reid, and F. A. Hegmann, Phys. Rev. B **79**, 193204 (2009).
6. J. Hebling, M. C. Hoffmann, H. Y. Hwang, K.-L. Yeh, and K. A. Nelson, Phys. Rev. B **81**, 035201 (2010).
7. H. Hirori, M. Nagai, and K. Tanaka, Phys. Rev. B **81**, 081305 (2010).
8. S. Watanabe, N. Minami, and R. Shimano, Opt. Express **19**, 1528 (2011).
9. A. Dienst, M. C. Hoffmann, D. Fausti, J. C. Petersen, S. Pyon, T. Takayama, H. Takagi, and A. Cavalleri, Nat. Photon. **5**, 485 (2011).
10. E. Balogh, K. Kovacs, P. Dombi, J. A. Fülöp, G. Farkas, J. Hebling, V. Tosa, and K. Varju, Phys. Rev. A **84**, 023806 (2011).
11. J. Hebling, J. A. Fülöp, M. I. Mechler, L. Pálfalvi, and C. Tőke, presented at the 33rd International Free Electron Laser Conference, Shanghai, China, MOPC13 (2011).
12. J. Hebling, G. Almási, I. Z. Kozma, and J. Kuhl, Opt. Express **10**, 1161 (2002).
13. H. Hirori, A. Doi, F. Blanchard, and K. Tanaka, Appl. Phys. Lett. **98**, 091106 (2011).
14. J. A. Fülöp, L. Pálfalvi, G. Almási, and J. Hebling, Opt. Express **18**, 12311 (2010).
15. J. A. Fülöp, L. Pálfalvi, M. C. Hoffmann, and J. Hebling, Opt. Express **19**, 15090 (2011).
16. M. I. Bakunov, S. B. Bodrov, and E. A. Mashkovich, J. Opt. Soc. Am. B **28**, 1724 (2011).
17. S. Klingebiel, C. Wandt, C. Skrobol, I. Ahmad, S. A. Trushin, Z. Major, F. Krausz, and S. Karsch, Opt. Express **19**, 5357 (2011).
18. M. C. Hoffmann, K.-L. Yeh, J. Hebling, and K. A. Nelson, Opt. Express **15**, 11706 (2007).
19. J. Hebling, A. G. Stepanov, G. Almási, B. Bartal, and J. Kuhl, Appl. Phys. B **78**, 593 (2004).
20. K. Wynne and J. J. Carey, Opt. Commun. **256**, 400 (2005).